Received: 21 October 2019 | Revised: 21 May 2020 | Accepted: 21 May 2020

DOI: 10.1002/er.5662

SPECIAL ISSUE RESEARCH ARTICLE

INTERNATIONAL JOURNAL OF ENERGY RESEARCH WILEY

Coupling a Stirling engine with a fluidized bed combustor for biomass

Francesco Saverio Marra[1] | **Francesco Miccio**[2] | **Roberto Solimene**[1] | **Riccardo Chirone**[1] | **Massimo Urciuolo**[1] | **Michele Miccio**[3]

[1]Institute for Research on Combustion (CNR-IRC), Naples, Italy

[2]Institute of Science and Technology for Ceramics (ISTEC-CNR), Faenza (RA), Italy

[3]Department of Industrial Engineering DIIn, University of Salerno, Fisciano (SA), Italy

Correspondence
Francesco Miccio, Institute of Science and Technology for Ceramics (ISTEC-CNR), via Granarolo 64, 48018, Faenza (RA), Italy.
Email: francesco.miccio@cnr.it

Summary

The paper deals with the integration between a kinematic Stirling engine and a fluidized bed combustor for micro-scale cogeneration of renewable energy. A pilot-scale facility integrating a 40 kW_t combustor and a γ-type Stirling engine (0.5 kW_e) was set up and tested to demonstrate the feasibility of this solution. The Stirling engine was installed at a lateral wall of the combustor in direct contact with the fluidized bed region. An experimental campaign was executed to assess the performance of the innovative integrated system. The experimental results can be summarized in: (a) very high combustion efficiency with biomass feeding, (b) elevated heat transfer rate to the engine, (c) a relatively small share (about 2 kW_t) transferred to the engine from the thermal power generated by the combustor (around 13 kW_t), (d) conversion to electric power close to the upper limit of the engine, (e) limited impact of the Stirling engine on the fluidized bed behavior, for example, temperature. From the analysis of measured variables, the dynamics is dominated by the fast response of the Stirling engine, which rapidly reacts to the slow changes of the fluidized bed combustor regime: the dynamic response of the tested facility as a thermal system was slow, the time constant being of the order of 10 minutes.

KEYWORDS

biomass, fluidized bed combustion, mathematical modeling, micro-generation, Stirling engine, system dynamics

1 | INTRODUCTION

Biomass is a widely available energy resource that can contribute to satisfy the increasing demand, in particular in emerging countries having low net emission impact on the greenhouse effect.[1] Biomass is also recognized as an ideal feedstock for supplying small and local installation, that is micro-generation in off-grid configuration, thanks to the worldwide availability of biomass in rural and mountain areas.[2] So far, the micro-generation of electricity (below 50 kW_e) includes devices based on compact generators, fueled by natural gas/diesel/gasoline, or powered by photovoltaic/wind devices.[3] Although small biomass burners (up to 100 kW_t) have large diffusion for residential heating, cooking and small industrial applications, cogeneration of electricity along with heat in such equipment is difficult because of technological and economic barriers. In general, this issue requires apparatuses that are not easily down scalable (eg, ORC, steam turbines) or have a very low conversion efficiency (eg, steam engines).[4] Recent developments of the Stirling engine (SE),[5] in particular in the free-piston configuration, allow to design biomass cogeneration systems even at a scale lower than 10 kW_e. Although coupling a biomass burner

with a Stirling engine was already attempted in the past, reliable operation has been hardly achieved. The basic idea was to place the hot exchanger of the SE in direct contact with the flame generated by the biomass combustion, in order to maximize the heat transfer between the flame and the working fluid in the engine. Unfortunately, such configuration turns out scarcely reliable in case of conventional biomass combustors (eg, grate systems), because of irregular flames, lower temperature, and soot formation in comparison with a premixed gas burner.[6] Therefore, in usual design configurations of biomass-fueled burners coupled with SE, heat is recovered from the exhaust gases, while the biomass combustion takes place in a separated chamber, such as a grate or brazier used for chips/pellet combustion.[7] A major drawback of this concept is the likely growth of carbon/ash deposits on the heat exchanger of the engine, leading to progressive reduction of the heat transfer rate from the flue gases to the SE[8] and, consequently, of the conversion efficiency and device reliability. In particular, Cardozo et al[9] reported ash accumulation on the surface of the SE heat exchanger, causing a decrease of the hot-side temperature after several cycles of wood pellet operation. Nevertheless, prototypes or near-commercial integrated modules based on a biomass-combustor and a Stirling engine have been developed in last decades.[9-13] A theoretical analysis was proposed by Harrod et al[14] for a small cogeneration plant based on biomass combustion and Stirling engine, highlighting that use of low-cost fuels (eg, waste wood) and the effectiveness of the Stirling engine are key factors for decreasing the operation costs and achieving profitable operation. A 9.5 kW_e wooden pellet-fueled Stirling for a district heating plant was considered by Alanne et al[15] in a techno-economic analysis leading to controversial conclusions about the suitability of low efficiency SE in a perspective of zero energy standards for buildings.

The integration between a Stirling engine and a fluidized bed combustor (FBC) represents a viable alternative option for overcoming most of problems experienced during biomass firing, thanks to the very clean combustion, along with the large effectiveness in heat transfer in fluidized beds.[16] Furthermore, the fluidized bed (FB) exerts self-cleaning of the internals in direct contact with the fluidized particles, preventing the formation of deposits on the heat transfer surfaces or removing locked particles in interstices between the tubes of heat exchanger bundle.[17] Therefore, coupling a fluidized bed combustor with a Stirling engine allows attaining heat transfer coefficients higher than those in a flame[18] in a very reliable configuration. This idea was conceptually explored by Miccio[19] and Angrisani et al[20] for the implementation of a cogeneration plant based on a small-scale FBC coupled with a kinematic SE. First experimental results obtained following such an approach, that is, a 40 kW_t bubbling fluidized bed equipped with an El.Ma (Electronic Machining, Riva del Garda, Italy) Stirling engine, were reported by Urciuolo et al,[21] achieving the maximum power of 500 W_e with reliable operation of the fluidized bed combustor.

This paper reports on further experimental results and modeling investigations from the operation of the above-mentioned integrated plant. In particular, the main features characterizing the observed dynamics of the fluidized bed combustor were obtained by means of a standard analysis as a linear dynamic system. In addition, a lumped-parameter dynamic mathematical model was developed and used for the quantitative description of the observed phenomenology.

2 | METHODS AND MATERIALS

2.1 | Fluidized bed combustor

The schematic of the fluidized bed combustion plant with nominal power of 40 kW_t used for the experimental investigation is shown in Figure 1. The air fluidization unit was designed with a square cross section and built in stainless steel with two parts: the bottom trunk (290 × 290 mm) was 1350 mm high, the upper trunk has

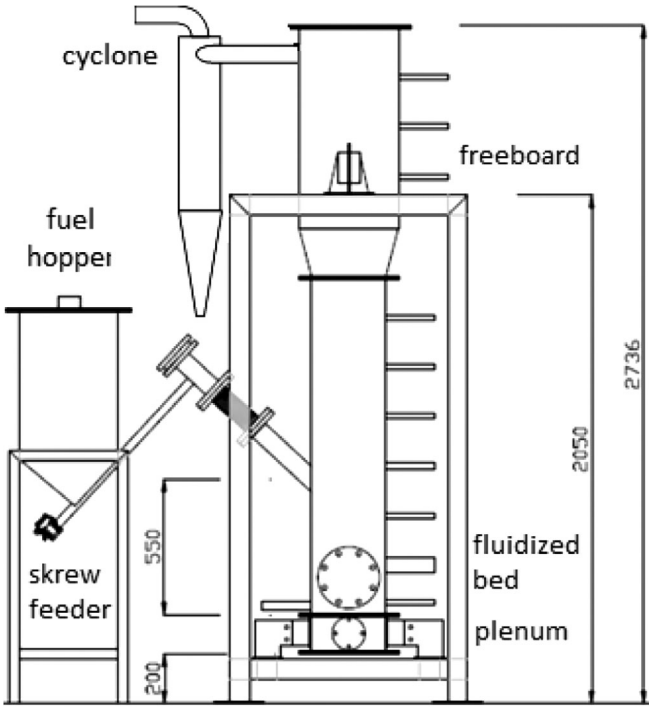

FIGURE 1 Schematic of the experimental plant with a square section (290 × 290 mm) fluidized bed combustor

a larger size (382 × 382 mm) and a height of 1012 mm, including a pyramidal connection (Figure 1). The fluidization column was insulated with ceramic fiberboards, able to withstand temperatures up to 1000°C, enclosed in a protective aluminum shell. The air fluidization stream, regulated by a globe valve, was supplied to the plenum (150 mm high) at the bottom of the fluidization column, equipped with an 8 mm thick perforated plate distributor, having 676 holes, 1 mm ID. The primary air was measured by means of a Brooks electronic flowmeter mod. SLA5800 (0-100 Nm^3/h). The feeding system for solid fuel (wood chips and pellets) comprised a sealed hopper with a volume of 100 L, a 25 mm ID screw feeder, an electric actuator, and an inclined side port for overbed feeding, at an elevation of 800 mm from the air distributor. An inverter allowed the fine regulation of the screw rotation speed. The primary abatement of particulate solids was carried out by a cyclone (ID = 98 mm), accomplishing the separation of entrained particles with a diameter up to 10 μm. A secondary fiber/ceramic filter was installed in sequence. Samples of fine solids were collected at the cyclone dipleg and the filter case exit.

The combustor was equipped with an electric air preheater (mod. Sylvania Max 10 kW) for fast heating-up of the fluidization stream to a temperature around 600°C. Along the fluidization column, four K-type thermocouples were installed at elevations of 60, 410, 810, and 1760 mm, respectively, from the air distributor; two electronic pressure transducers (250 mbar full scale) were connected to ports located at 410 and 810 mm, respectively, from the air distributor. A gas analyzer for O_2, CO, CO_2, and NO (mod. ABB AO-URAS26) monitored the flue gas composition at the exit port of exhausts. The bed (total inventory of 45 kg) was made by silica sand with average size of 500 μm and minimum velocity for fluidization of 0.30 m/s at room temperature. The fluidization velocity was kept in the range 0.25 to 0.30 m/s, at average operating bed temperature of 830°C. This latter was controlled by changing the fuel-feed rate and, consequently, the excess air ratio.

2.2 | Stirling engine

The Stirling engine was manufactured by El.Ma Electronic Machining (Riva del Garda, Italy), with a nominal electric power of 500 W. It is a two-cylinder kinematic machine in γ-type configuration. The drawings of the Stirling engine are shown in Figure 2, with indication of principal quotes. The main parts of the engine are: (a) the expansion cylinder, where there is the evolution of the gas moved by the displacer (95 mm diameter); (b) the compression cylinder, in which the power piston (75 mm diameter) translates, generating the power for sustaining the whole cycle; (c) the regenerator, consisting of a metallic sponge that acts as an intermittent heat storage device, increasing the engine performance (total volume 321 mL); (d) the cold-side heat exchanger, consisting of a cooling liquid (water) circuit, moved by a dedicated pump; (e) the hot-side heat exchanger, which provides the thermal energy to the working fluid, formed by No. 20 U-tubes 8 mm OD and 320 mm long, as drawn in Figure 2A (left side). The nominal pressure of the SE working fluid (ie, N_2) is 8 bars. The engine was pneumatically/electrically connected to a central unit for monitoring and controlling its operation by means of a dedicated software.

The Stirling engine was horizontally installed in the bottom section of the fluidized bed chamber at an

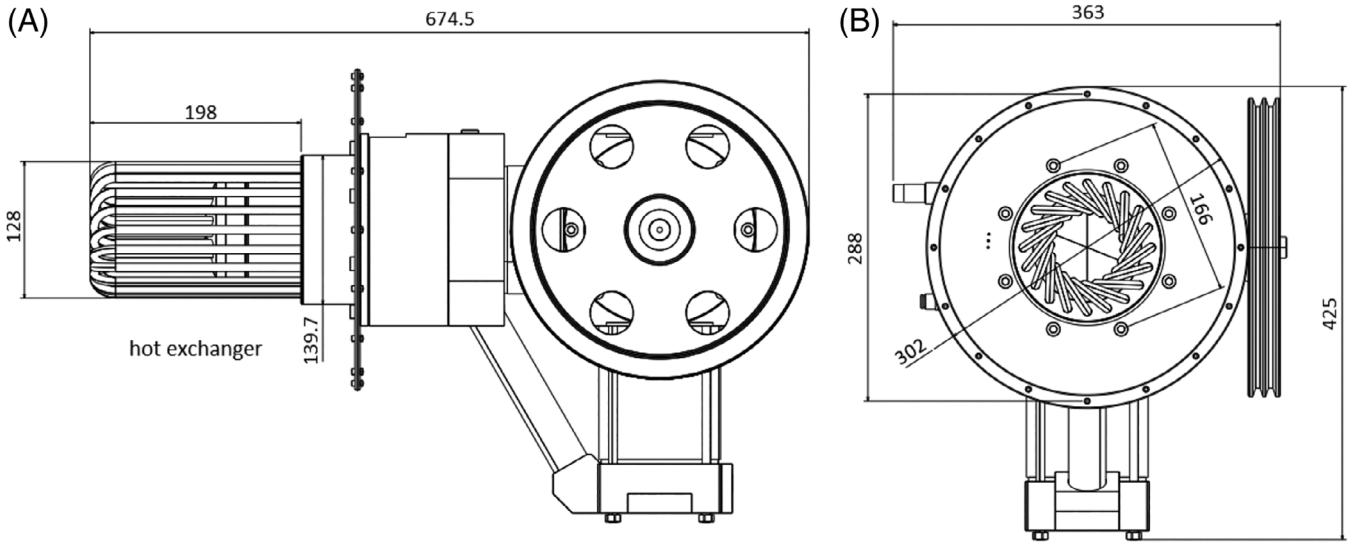

FIGURE 2 Drawings of the Stirling engine; lateral view A, frontal view B

elevation of 206 mm from the air distributor. The hot exchanger of the engine was fitted throughout a 5″ circular flange with a protrusion of 13 mm with respect to the internal combustor wall. A 5″ ID AISI316 flexible hose, a spring-compensator and a calibrated counterweight, allowed to compensate the differential dilatations between burner and engine, as well as to damp the vibrations during the engine operation. The clearance between the tube bundle of the exchanger and the flexible hose ensured presence of fluidized bed particles in contact with the whole surface of the heat exchanger.

2.3 | Fuel

Commercial pine-wood pellets were used as fuel during the tests, as they allowed a more reliable operation of the screw feeder and a more compact design of the fuel storage devices with respect to other biomass feedstock. The properties of the pellets are summarized in Table 1. Proximate and ultimate analyses were carried out by means of a TGA 701 LECO thermogravimetric analyzer and a CHN 2000 LECO equipment, respectively.

3 | EXPERIMENTAL RESULTS

From a qualitative point of view, there was no impact on the fluidized bed combustor behavior due to the presence of the SE exchanger. The time profiles of pressure measured in the fluidized bed were very similar to those obtained in tests without the presence of the Stirling engine, as shown in Figure 3. It is worth recalling that the SE exchanger protruded into the transversal bed section for 13 mm at maximum, thus, the disturbance on the bed hydrodynamics was limited.

TABLE 1 Proximate analysis, ultimate analysis, and heating value of the fuel

Proximate analysis	**% wt**
Moisture	6.6
Fixed carbon	16.3
Volatiles	76.6
Ash	0.4
Ultimate analysis	**% wt (dry base)**
C	50.0
H	6.3
N	<0.1
O by diff.	43.7
LHV, MJ kg^{-1}	19.6

The combined FBC-SE system has been operated dozens of hours in both no-running and running mode of the Stirling engine. There was no evidence of problems, such as local overheating, bed defluidization, particle sintering, bypass phenomena of evolved gas, etc. In particular, no damage or erosion of the SE hot exchanger was observed, from periodic inspection of the device.

Figure 4 shows the time profiles of the temperature measured by the thermocouples inserted in the combustion vessel with operation of the Stirling engine and without it. It clearly appears that during the engine operation (ie, 600 rpm), there was a cooling effect and the bed temperature declined to a lower level. Under the test conditions, the high-temperature level was around 840°C (no SE operation), whereas the low-temperature level approached 820°C.

At steady-state test conditions, the fuel-feeding rate was 3.1 ± 0.1 kg/h, with a corresponding thermal power of 12.5/13.3 kW, and an excess air ratio oscillating in a range as narrow as 2.0/2.2. The concentration of the main gaseous species in the exhausts is reported in Table 2, demonstrating that very efficient and clean combustion occurred, with low emissions of both carbon monoxide and nitrogen oxide.

Concerning the SE operation, the revolution speed of the engine did not change during operation, thanks to the efficient internal control loops driven by its central unit, and maintained the value of 600 rpm. The temperature measured by a dedicated thermocouple in the hot exchanger of the SE, not reported here, was only few degrees lower than T_1, indicating effective mixing of the fluidized bed solids, even in presence of internals.

Figure 5 shows the time profiles of the electric (W_e) and cooling (W_c) power during the operation of the Stirling engine (same test of Figure 4). The cooling power was calculated by Equation (1), on the basis of data provided by the El.Ma monitoring/controlling software,

$$Q_c = \dot{M}_w \, (T_{w,o} - T_{w,i}) \, c_p, \tag{1}$$

where $\dot{M}_w$ is the mass flowrate, $T_{w,o}$ and $T_{w,i}$ are the outlet and inlet temperature, and c_p is the specific heat of the cooling water.

The total power W_t, representing the heat transfer rate from the fluidized bed to the Stirling engine, is computed as the sum $W_t = W_e + W_c$. The noise in the W_c diagram (Figure 5) was likely due to the little difference between $T_{w,o}$ and $T_{w,i}$ as well as the periodic refilling of the cooling tank with fresh water. Actually, during the first-time interval, that is, 250 to 350 minutes, the fluidized bed temperature was still increasing after start-up from 700 to 800°C. Nevertheless, an electric power with

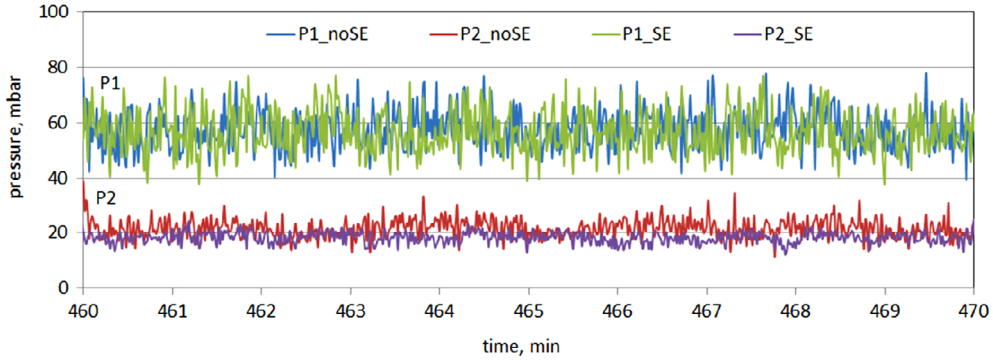

FIGURE 3 Time profiles of the pressure measured by P_1 and P_2 transducers in absence (noSE) and presence (SE) of the Stirling engine under similar fluidization conditions ($T = 800°C$) [Colour figure can be viewed at wileyonlinelibrary.com]

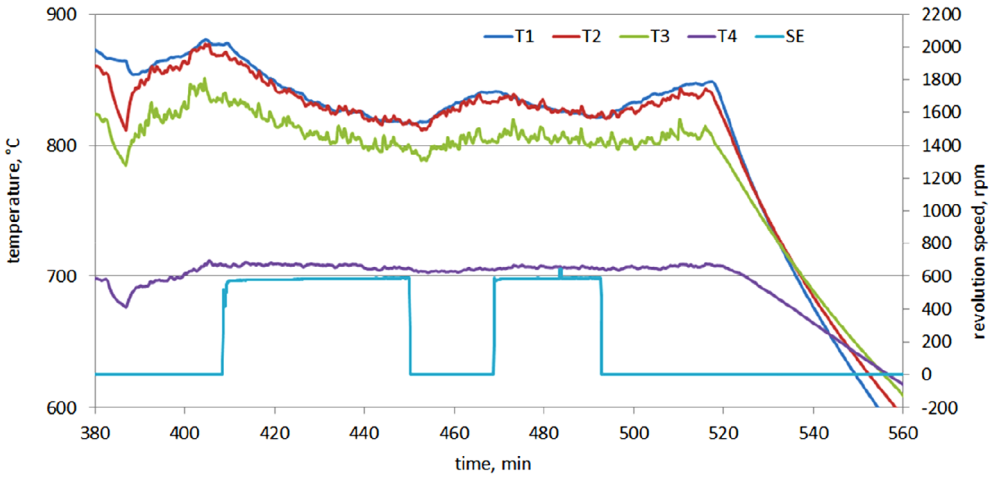

FIGURE 4 Time-resolved profiles of bed (T_1-T_2 thermocouples) and freeboard (T_3-T_4 thermocouples) temperatures and revolution speed of the Stirling engine as a consequence of two ON/OFF switches of the Stirling engine [Colour figure can be viewed at wileyonlinelibrary.com]

TABLE 2 Range of variation for main fluidized bed combustor measured variables during Stirling engine operation

T_b, °C	800-870
O_2, % vol. (dry base)	10.0-12.0
CO_2, % vol. (dry base)	9.5-11.5
CO, ppm (dry base)	0-5
NO, ppm (dry base)	95-105
Excess air ratio, –	2.0-2.2

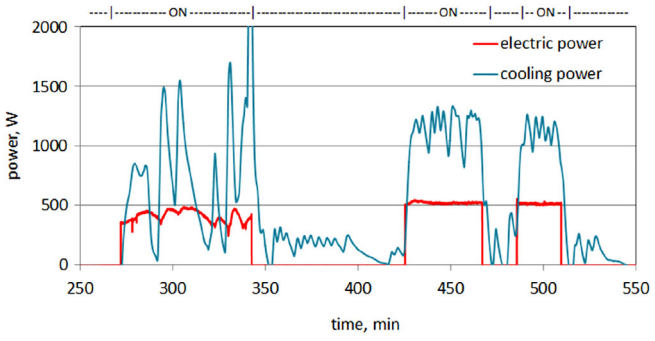

FIGURE 5 Time-resolved profiles of the instantaneous power (either electric or cooling) as a consequence of ON/OFF switches of the Stirling engine [Colour figure can be viewed at wileyonlinelibrary.com]

an average value of about 400 W was generated. In the two next operation intervals, when the FBC temperature exceeded 800°C, a net electric power slightly above 500 W was generated, with an SE conversion efficiency of 30%. This latter was calculated as the ratio between the electric power and the total power transferred from FBC to SE. It is worth noting that the temperature of the cooling water was kept between 20°C and 30°C, in order to maximize the conversion efficiency into electricity. The efficiency in electric generation with respect to the input fuel power was 3.8%, as consequence of the large nominal power of combustor (up to 40 kW_t).

4 | MAIN FEATURES OF THE OBSERVED DYNAMICS

Based on the above experimental findings, the FB temperature T_b turns out the process variable the pattern of which adequately represents the dynamics of the combined FBC-SE system.

The main features of the bed temperature dynamics have been captured by taking the observed dynamic data on T_b and carrying out a suitable mathematical fitting of them. To this end, a simple lumped-parameter model,[20]

that is, the First-Order Plus Dead Time (FOPDT), was reasonably implemented to approximate the dynamics of the bed temperature T_b:

$$\tau_P \frac{dT_b(t)}{dt} + T_b(t) = K_P \mathrm{u}(t - t_d) \quad (2)$$

where u(t) is a known input variable that is subjected to a prefixed change with time (ie, in this case, the SE revolution speed), and the unknown parameters are the process gain K_P, the process time constant τ_P, and the apparent dead time t_d. The observed process data were the T_1 data series in Figure 4.

Figure 6 displays the graphical results of the FOPDT model fitting to the experimental data when the input variable has undergone a sequence of step-up and step-down changes with time, in other words, when the Stirling engine has been switched on and off in a given sequence during the test (see Figure 4).

Table 3 reports the values of the parameters characterizing the dynamics. First of all, the estimated FOPDT parameters exhibit an excellent goodness of fit as demonstrated by the values of the linear correlation coefficient, R^2, that always exceed 0.993. Obviously, a truly linear dynamic system presents the same values of the FOPDT parameters independently of the step size by which the input variable is varied[22]; conversely, a shift in the value of a FOPDT parameter is an indication of non-linearity in the tested dynamical system. This approach was already applied with success in the analysis of time series during biomass combustion in a residential fluidized bed boiler.[23]

The process gain, K_p, which is the ratio between the overall variation of the observed process variable and the step size of the input variable, turns out negative. Hence, the bed temperature dynamics is characterized by a "reverse acting" response to the switch of the Stirling engine operation. Obviously, when a thermal power is removed by the Stirling engine with a cooling effect on the bed operated at constant fuel-feed rate, the bed temperature falls down. The actual values of K_p are comparable in magnitude, irrespective of the direction of the step change (ie, up or down mode), with the exception of $K_p = -0.117$°C/rpm as calculated for the step up at the test time of 408.5 minutes (see Figure 6A). However, the authors believe that this is to be considered a result of data scattering and not an indication of non-linearity.

The process time constant, $\boldsymbol{\tau}_P$, which is an indicator of the system celerity to adjust itself after a dynamic change in an input variable, shows a limited variability in the range 11 to 19 minutes, but strictly keeps the same order of magnitude irrespective of the direction of the step change. It is worth noting that the thermal dynamics

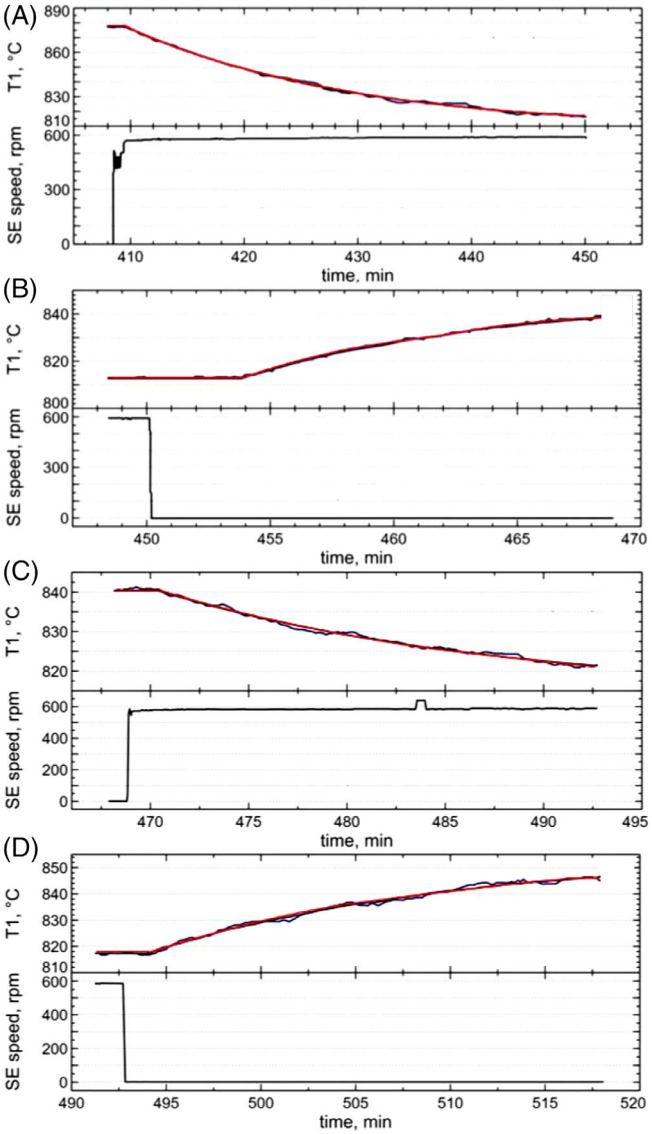

FIGURE 6 The First-Order Plus Dead Time model fitting (red) of the bed temperature data series (black) providing the unknown parameters characterizing the dynamics upon status change of SE: engine ON (A, Cc); engine OFF (B, D) [Colour figure can be viewed at wileyonlinelibrary.com]

of the fluidized bed is very slow. This is due to the thermal inertia of the bed solids inventory, acting as a "system capacitance": in other words, the achievement of a new steady state for FB temperature following the on/off switch of the Stirling engine takes a time that is about $4\boldsymbol{\tau}_P$.[22]

The process dead time t_d, which in principle stands for a transportation lag in the temperature measurement of the system, is quite low, that is, in the order of 1 minute, confirming that the bed temperature dynamics is not affected by a pure delay, as expected for such a process system. The exception is t_d = 3.7 minutes as

TABLE 3 Values and goodness of fit for the First-Order Plus Dead Time parameters characterizing the dynamics of the bed temperature

State variable	Test code	Step time min	Step mode	K_p °C/rpm	τ_p min	t_d min	R^2
T_b	08.02.18-I	408.5	Up	−0.117	19.0	1.1	0.9974
	08.02.18-II	468.0	Up	−0.0441	16.8	1.5	0.9936
	08.02.18-I	450.0	Down	−0.0553	10.6	3.7	0.9968
	08.02.18-II	492.7	Down	−0.0612	16.6	1.2	0.9930

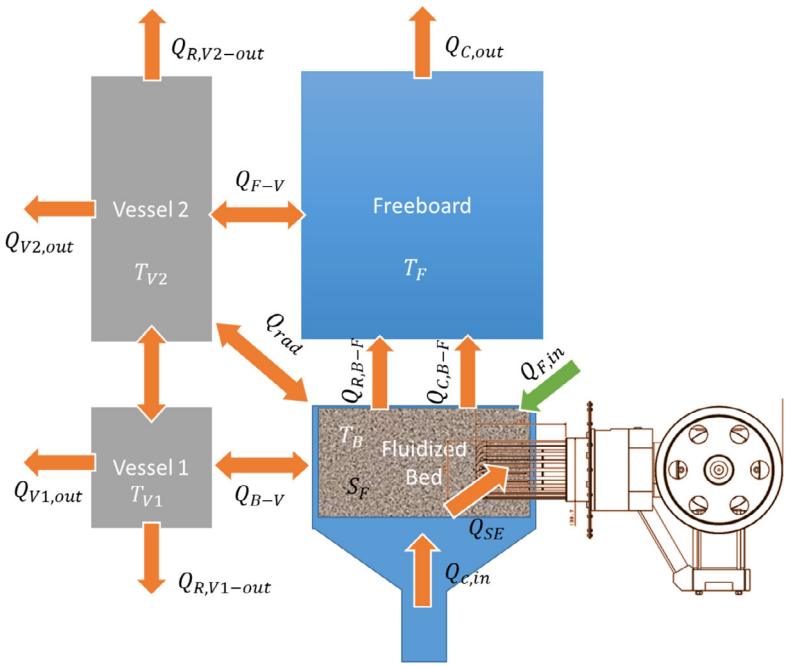

FIGURE 7 Schematic of the lumped-parameter dynamic model. Heat flows: $Q_{F,in}$: fuel enthalpy; Q_{SE}, Stirling engine heat transfer; $Q_{R,B\text{-}F}$, bed-freeboard heat (radiation); $Q_{B\text{-}V}$, bed-insulation transfer (conduction); Q_{rad}, bed-insulation transfer (radiation); $Q_{R,V2out}$, freeboard insulation loss (radiation); $Q_{V2,out}$, freeboard insulation loss (convection); $Q_{C,in}$, combustion air (convection); $Q_{C,B\text{-}F}$, bed-freeboard heat (convection); $Q_{C,out}$, exhausts enthalpy (convection); $Q_{F\text{-}V}$, freeboard-insulation transfer (conduction); $Q_{R,V1out}$, bed insulation loss (radiation); $Q_{V1,out}$, bed insulation loss (convection) [Colour figure can be viewed at wileyonlinelibrary.com]

calculated for the step down at the test time of 450 minutes. Again, the authors believe that this is to be considered a result of data scattering and not an indication of non-linearity in system dynamics.

5 | MODELING

A model, based on a reactor network, has been adopted to numerically simulate the experimental results and gain a better understanding of the interaction between the combustor behavior and the engine performances. The model was presented in Angrisani et al[20] and Bizon et al.[24] Here, for the sake of brevity, only the main energy balance equations are reported.

Figure 7 illustrates the reactor network adopted to describe the energy interactions between the main functional components of the system and all energy fluxes linking the different blocks. The core of the network is represented by the fluidized bed combustor (B), where the main phenomena occur: heat accumulation in fluidized sand, fuel burning, and heat transfer to the Stirling engine (SE). The bed exchanges heat with all other blocks, whereas the Stirling engine is represented by a separate block.[20] The control volume for the bed is defined by the surface surrounding the fluidized bed. The fluidized bed is only a part of the combustor, which includes metal walls and insulating layers, subdivided into two portions, one adjacent to the bed (V1) and the other to the freeboard (V2). The remaining block is the freeboard volume (F). The balance equations are written under the following assumptions: lumped properties in each of the parts composing the block model, which implies perfect mixing of fluid and solids in each part; constant heat capacities; pseudo homogeneous bed (same temperature for solid- and gas-phase in the bed); constant pressure in each block, with changes in density and specific heats only due to composition and/or temperature changes. Therefore, the total variation of energy in the fluidized bed control volume E_b is approximated as:

$$\frac{dE_b}{dt} = \frac{d}{dt}\left[\rho_g V_g C_{pg}(T_b - T_0) + \rho_s V_s C_{ps}(T_b - T_0)\right] \approx \rho_s V_s C_{ps}\frac{dT_b}{dt} = m_s C_{ps}\frac{dT_b}{dt}, \quad (3)$$

where subscripts g and s refer to gas and solid phase, respectively. The approximation adopted in Equation (3) corresponds to say the energy in the system can only accumulate in the solid. The balance equation for the fluidized bed is then given by:

$$m_s C_{ps}\frac{dT_b}{dt} = Q_{c,\text{in}} + Q_{F,\text{in}} - Q_{\text{SE}} - Q_{B-V} - Q_{C,B-F} - Q_{R,B-F} - Q_{\text{rad}} + S_F + S_{ht}. \quad (4)$$

Two energy source terms are included: S_F takes into account the power added by the biomass combustion, taking into consideration the effective bed conditions, whereas S_{ht} takes into account the power supplied by the heater for the start-up of the plant. The balance equation for the freeboard region, with analogous assumptions, is given by:

$$m_g C_{pg}\frac{dT_f}{dt} = Q_{C,B-F} + Q_{R,B-F} - Q_{C,\text{out}} - Q_{F-V}. \quad (5)$$

The change in the energy in the two vessel portions can be similarly expressed as:

$$m_{V1} C_{p,\text{vess}}\frac{dT_{V1}}{dt} = Q_{B-V} - Q_V^k - Q_{V1,\text{out}} - Q_{R,V1-\text{out}}, \quad (6)$$

$$m_{V2} C_{p,\text{vess}}\frac{dT_{V2}}{dt} = Q_{F-V} - Q_V^k - Q_{\text{rad}} - Q_{V2,\text{out}} - Q_{R,V2-\text{out}}, \quad (7)$$

In these expressions, Q terms refer to energy fluxes exchanged between the different blocks of the network or with the external environment as illustrated in Figure 7. All the expressions for the terms at the right-hand side of Equations (4) to (7) are detailed in Reference 24. This set of ordinary differential equations is then completed with its relevant initial conditions.[24] A simple explicit Euler scheme was effectively implemented for the numerical integration of the model equations.

The model results are illustrated in Figure 8 (left), where time-resolved profiles of the temperatures of the bed T_b and of the freeboard T_f are reported for three different operating conditions: (a) those investigated in the present study (top); (b) using a more powerful Stirling engine (middle); and (c) using a more powerful Stirling engine and increasing the input fuel power (bottom). A comparison of the predicted temperature profiles with the experimental results (see Figure 4) shows a satisfactory agreement, including the ability to catch the effect of the activation of the Stirling engine on the bed temperature. Increasing the SE power from 497 to 2773 W determines a more pronounced reduction of bed temperature even to values lower than 700°C (see Figure 8, middle and left), which is not compatible with good FBC performances in terms of emissions. To avoid dramatic temperature reductions, a proper control strategy of bed temperature has to be established to take into account, at the same time, the thermal dynamics of the fluidized bed and the operation dynamics of the SE. Figure 8 (bottom) shows the results obtained when the temperature reduction is contrasted by means of a step increase of the fuel-feed rate. In this case, the bed temperature can be kept at values higher than 750°C whatever condition for SE operation is considered. Also shown in Figure 8 (right), for the three investigated conditions, are the budgets of all power terms in Equation (4) that allows appreciating which terms are more sensitive to the coupling between the FBC and the SE. It is recognizable that, at the activation of the Stirling, a significant share of the energy from the biomass combustion shifts to heat the SE (Q_{SE}), generating power (P_{SE}). The corresponding decrease of the bed temperature also affects the radiation losses from the bed while the energy leaving the bed with the exhausts remains almost unvaried. The bed is indeed able to act as a thermal accumulator that makes slowly variable the energy transferred to the SE also in presence of fluctuations of the bed temperature, a circumstance beneficial for the proper and efficient operation of the SE.

It is clear that the electric power, P_{el}, is only a very small fraction of the fuel energy available under the experimentally investigated conditions. Since the El.Ma SE presently coupled to FB in the experimental rig appears to be undersized with respect to the thermal power of the FB combustor, the present experimental results do not allow a proper exploitation of thermal energy conversion to electric power that would be expected by an effective combined FBC-SE concept. In order to move toward this latter direction, a first step would be that of replacing the El.Ma SE with a more powerful device, as finally demonstrated by the above simulation results. A second step is that of exploiting the power leaving the bed as hot exhaust gases, $Q_{C,B\text{-}F}$.

The application of an economizer in the freeboard, which allows to recover most of the available sensible heat for preheating the incoming air, would achieve a significant reduction of the fuel-feeding rate, thus increasing the excess air ratio or lowering the fluidization velocity. This effect has been the object of a theoretical investigation,[25] showing that the introduction of the economizer can effectively raise the share of fuel conversion into electric power. According to this study, the recovered power Q_r is expressed by Equation (8):

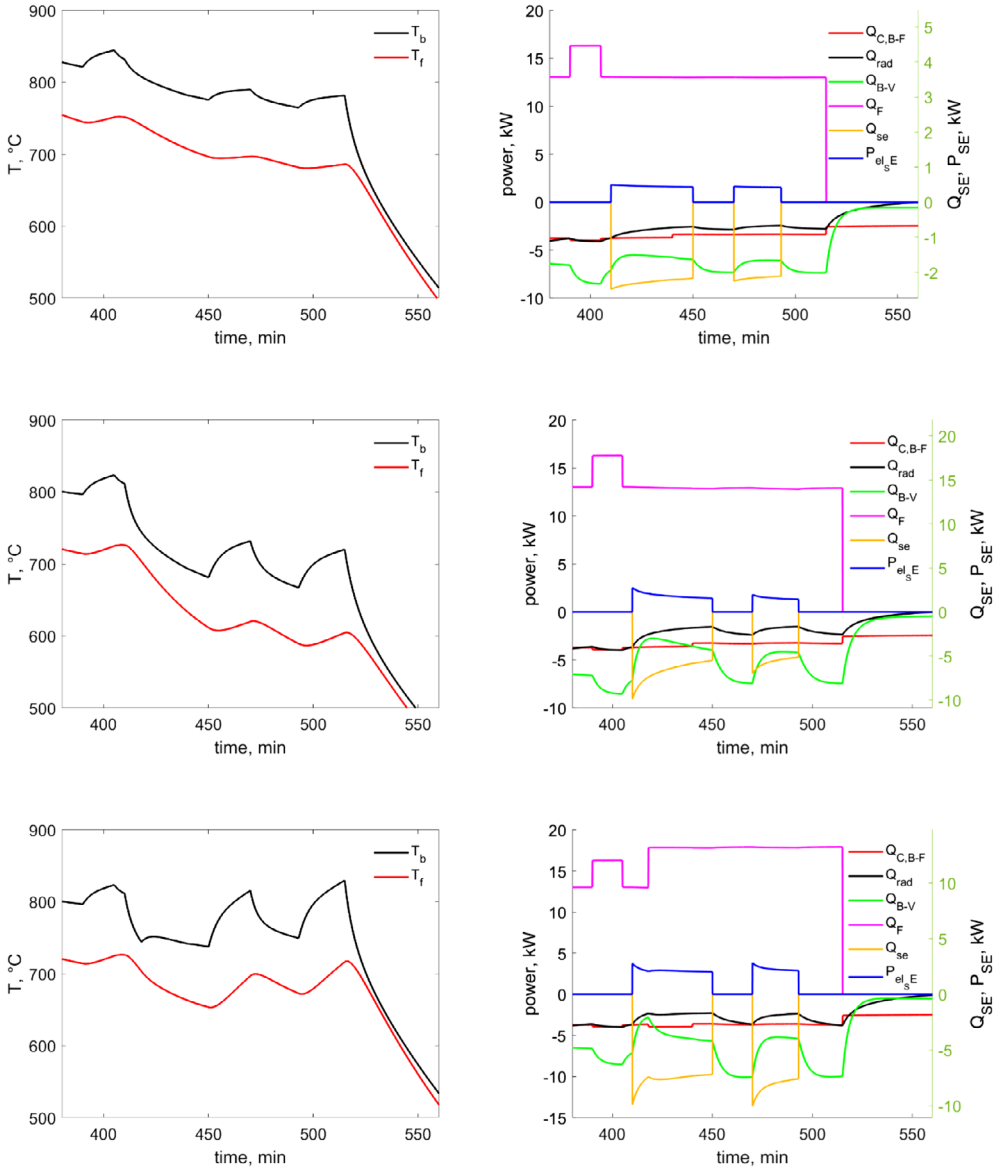

FIGURE 8 Simulation results: computed temperature profiles (left) and power budgets (right). Top: engine parameters corresponding to the El.Ma devise used in the experiments (max computed power is 497 W and max heat absorbed is 2488 W). Middle: engine parameters corresponding to a more powerful engine (max computed power is 2773 W and max heat absorbed is 9905 W). Bottom: engine parameters corresponding to a more powerful engine (max computed power is 2773 W and max heat absorbed is 9905 W) and an increased fuel-feed rate [Colour figure can be viewed at wileyonlinelibrary.com]

$$Q_r = A\rho_g U_g C_{pg}\left(T_{pr} - T_0\right) = A\rho_f U_f C_{pf}\left(T_b - T_f\right), \quad (8)$$

where U is the superficial gas velocity, A the bed cross section and subscript pr denotes the preheating state of the incoming fluidizing gas. After assuming constant thermal properties of the gaseous streams, at least in a first-analysis approach, the preheating temperature turns out linearly dependent on the exit temperature of exhausts T_f at constant bed temperature T_b:

$$T_{pr} = T_0 + \frac{\rho_g U_g C_{pg}}{\rho_f U_f C_{pf}}\left(T_b - T_f\right). \quad (9)$$

By considering the low heating value LHV of the fuel, the saved feed rate of fuel is:

$$\dot{M}_{sav} = \frac{\rho_f U_f C_{pf}\left(T_b - T_f\right)}{\mathrm{LHV}}. \quad (10)$$

The computations made for three different values of T_f (ie, 700°C, 600°C, and 500°C) showed that the saved fuel with respect to the case of no preheating (ie, the present experimental results) is 7, 14 and 21% wt, respectively. Correspondingly, the efficiency in electric generation was estimated to rise at least from 3.3 to 4.3%. The easier way to accomplish air preheating would be the insertion of a tubular heat exchanger in the freeboard, where beneficial effects are expected due to the residual particle loading of the exhaust gas stream and radiative heat transfer from the bed surface.[26]

As a final consideration, the integrated plant in the current configuration can be easily upgraded by installation of a second Stirling engine in an opposed position within the bed, allowing to double the generated electric

power. According to the experimental results shown in Figure 4 and model predictions (Figure 8), it is likely that no dramatic impact would occur by further extraction of thermal power from the bed, with an expected decrease in bed temperature of about 20°C.

6 | CONCLUSIONS

In this work, the soundness of combining a bubbling fluidized bed combustor and a Stirling engine, respectively, as a source and a sink of thermal power, in an integrated facility has been further demonstrated, with the added value of burning a biomass fuel and managing energy in a renewable way.

The experimental work yielded reliable operation of the integrated SE-FBC facility; superior heat transfer and no operating troubles of the SE heat exchange tubing; regular combustion and fluid-dynamic behavior of the fluidized bed in spite of the SE exchanger; gradual and limited drop of the bed temperature (around 20°C decrease) when the Stirling engine was activated at full electric power (ie, 0.5 kW); and smooth operation with feeding of commercial wood pellets.

A dynamic analysis of the combined FBC-SE facility has been driven by the experimental evidence that the overall dynamic behavior is dominated by the slow response of the fluidized bed to the ON/OFF switch of the engine operation and, consequently, the bed temperature T_b is the key state variable characterizing the dynamics. By adopting a simple First-Order Plus Dead Time approach to represent the dynamics, thanks to its approximation to a lumped-parameter model, the FBC-SE facility proved to act as a linear system, at least within the range of the tested operating conditions, with a "slow" process time constant, as determined in the range of 11 to 19 minutes.

Simulation and process performance prediction of the combined FBC-SE facility, either under transients or at steady state, have been carried out by means of a previously published mathematical model based on a reactor network. First, the simulation results, under the operating conditions of the combined FBC-SE facility tested in this work, were in a good agreement with experimental results, reproducing the effects of the Stirling engine ON/OFF switch. Second, the process performance prediction results proved that the currently tested FBC unit with a thermal power up to 40 kW_t could be equipped with a different and more powerful Stirling engine, that is, up to about 2.8 kW_e, without an impairing impact of the process performance of the biomass-fired fluidized bed combustor. In particular, results of model predictions showed that the FB combustor could be run at a bed temperature of 750°C, still a favorable temperature for a clean and reliable FBC operation, while having the more powerful Stirling engine switched on and suitably increasing the fuel-feed rate; in this case, the control strategy of the thermal regime of the combined FBC-SE facility would be based on fuel rate manipulation.

The tested FBC-SE facility opens perspectives to the concept of micro-scale cogeneration of renewable energy, upon an improvement in the combustor design (eg, heat recover for air preheating), number of coupled Stirling engines and application of more powerful devices (eg, free piston). On this basis, an off-grid plant based on FB-SE coupling would be feasible for remote applications (eg, in emergency situations).

NOMENCLATURE

A	fluidized bed section, m^2
c_p	specific heat, J $(kg°C)^{-1}$
FB	fluidized bed
FBC	fluidized bed combustor
K_p	process gain, –
LHV	low heating value of the fuel, kJ/kg
m	mass, kg
$\dot{M}$	mass flow, kg s^{-1}
$\dot{M}_{sav}$	mass flow rate of saved fuel, kg s^{-1}
P_{el}	electric power, W
P	pressure, mbar
Q	generic power, W
R^2	linear correlation coefficient, –
S	input power, W
SE	Stirling engine
T	temperature, °C
U	velocity, m/s
V	volume, m^3
W	power, W
t	time, min
t_d	process dead time, min
U	gas velocity, m/s

GREEK SYMBOLS

ρ	density, kg m^{-3}
τ_P	time constant, min

SUBSCRIPTS

b, B	bed
c	cooling
e	electrical
F	freeboard
f	exhausts
g	gas

ht	heater
I	inlet
o	outlet
pr	preheater
s	solid
t	total
V	vessel

ORCID

Francesco Saverio Marra https://orcid.org/0000-0003-4231-5652
Francesco Miccio https://orcid.org/0000-0003-0643-6721
Roberto Solimene https://orcid.org/0000-0001-8091-3501
Riccardo Chirone https://orcid.org/0000-0001-5404-4728
Massimo Urciuolo https://orcid.org/0000-0002-9386-3053
Michele Miccio https://orcid.org/0000-0001-8549-1504

REFERENCES

1. Booth MS. Not carbon neutral: assessing the net emissions impact of residues burned for bioenergy. *Environ Res Lett*. 2018;13:035001.
2. World Energy Council. *World Energy Resources 2016*. London, England: World Energy Council; 2016. ISBN: 9780946121588.
3. Kosmadakis G, Karellas S, Kakaras E. Renewable and conventional electricity generation systems: technologies and diversity of energy systems. In: Michalena E, Hills JM, eds. *Renewable Energy Governance*. London: Springer-Verlag; 2013:9-30.
4. Prasad SB. Steam engine characteristics and theoretical performance. *Energy Convers Manag*. 1993;34(12):1323-1333.
5. Walker F. *Stirling Engines*. Oxford, England: Clarendon Press; 1980.
6. Glassman I, Yetter RA, Glumac NG. Chapter 9 - Combustion of nonvolatile fuels. In: Glassman I, Yetter RA, Glumac NG, eds. *Combustion*. 5th ed. London, UK: Academic Press, 2014:477-536.
7. Bain RL, Overend RP. Biomass for heat and power. *For Prod J*. 2002;52:12-19.
8. Vos J. Biomass energy for heating and hot water supply in Belarus. Contract Report (BYE/03/G31), BTG; 2006.
9. Cardozo E, Erlich C, Malmquist A, Alejo L. Integration of a wood pellet burner and a Stirling engine to produce residential heat and power. *Appl Therm Eng*. 2014;73:671-680.
10. Podesser E. Electricity production in rural villages with a biomass Stirling engine. *Renew Energy*. 1999;16:1049-1052.
11. Jensen N, Werling J, Carlsen H, Henriksen UB, CHP from updraft gasifier and Stirling engine. Paper presented at: Proceedings of 12th European Biomass Conference; 2002;726-729.
12. HighBio Project. In: Lassi U, Wikman B, eds. *Biomass Gasification to Heat. Electricity and Biofuels*. Kokkola, FI: HighBio Project Publication; 2011.
13. Keck T, Schiel W, Envirodish and Eurodish-System and Status. Paper presented at: Proceedings of ISES Solar World Congress; 2003.
14. Harrod J, Mago PJ, Luck R. Sizing analysis of a combined cooling, heating, and power system for a small office building using a wood waste biomass-fired Stirling engine. *Int J Energy Res*. 2012;36:64-74.
15. Alanne K, Paatero J, Beausoleil-Morrison I. Performance assessment of a Stirling engine plant for local micro-cogeneration. *Int J Energy Res*. 2012;36:218-230.
16. Basu P. *Combustion and Gasification in Fluidized Beds*. Boca Raton, MA: CRC Press, Taylor & Francis; 2006.
17. Klaren DG, Boer de EF. Self-cleaning fluidised bed heat exchangers for severely fouling liquids and their impact on process design. In: Mitrovic J, ed. *Heat Exchangers Basics Design Applications*. Rijeka, Croatia: InTech; 2012.
18. Chen JC, Transfer H. In: Yang W-C, ed. *Handbook of Fluidization and Fluid-Particle Systems*. New York, USA: Marcel Dekker, Inc; 2003.
19. Miccio F. On the integration between fluidized bed and Stirling engine for micro-generation. *Appl Therm Eng*. 2013;52:46-53.
20. Angrisani G, Bizon K, Chirone R, et al. Development of a new concept solar-biomass cogeneration system. *Energy Convers Manag*. 2013;75:552-560.
21. Urciuolo M, Chirone R, Marra FS, Solimene R. Power generation by Stirling engine during fluidized bed combustion of wood pellets. *Combust Sci Technol*. 2019;191:263-274.
22. Cooper DJ. *Practical Process Control*. Manchester, Connecticut, USA: Control Station Inc.; 2008.
23. Cammarota A, Chirone R, Miccio M, Solimene R, Urciuolo M, Dual-fuel fluidized bed combustor prototype for residential heating: steady-state and dynamic behavior. Paper presented at: Proceedings of the 20th International Conference on Fluidized Bed Combustion, Xian (CN); 2009:441-447.
24. Bizon K, Marra FS, Continillo G, Fast predictive model for design and optimization of a low emissions biomass fueled CHP system. Paper presented at: 23th European Biomass Conference and Exhibition; 2015.
25. Lombardi S, Bizon K, Continillo G, Marra FS, Vaglieco BM, Combined Heat and Power generation from a Stirling Engine coupled with a Fluidized Bed Combustor. Paper presented at: XXXVI Meeting of the Italian Section of the Combustion Institute, Isola di Procida (I); June 13-15; 2013.
26. Batu A, Selcuk N. Modeling of radiative heat transfer in the freeboard of a fluidized bed combustor using the zone method of analysis. *Turkish J Eng Env Sci*. 2002;26:49-58.

How to cite this article: Marra FS, Miccio F, Solimene R, Chirone R, Urciuolo M, Miccio M. Coupling a Stirling engine with a fluidized bed combustor for biomass. *Int J Energy Res*. 2020;44:12572–12582. https://doi.org/10.1002/er.5662